◎ 논 문
◎ Original Paper

DOI: http://dx.doi.org/10.5293/kfma.2020.23.1.015
ISSN (Print): 2287-9706

# 단일 채널 펌프 모델의 성능 및 내부유동 특성에 대한 임펠러 블레이드 두께의 영향

곽명* · 최영도**†

# Effect of Impeller Blade Thickness on the Performance and Internal Flow Characteristics of a Single Channel Pump Model

Ming Guo*, Young-Do Choi**†

*Key Words : Single channel pump(단일 채널 펌프); Blade thickness(블레이드 두께); Performance(성능); Internal flow characteristics (내부 유동 특성); Pressure fluctuation(압력맥동); Cavitation number(캐비테이션 수)*

**ABSTRACT**

The single channel pump, which is widely used as a typical kind of sewage pump. Because of the special structure, it can reduce the damage of transportation substances. Therefore, it is possible to be employed for the transportation of alive fish and shrimp. In this study, a three dimensional (3D) modeling of single channel pump model was established by following the basic hydraulic design process. The blade thickness can be changed by modifying the outlet angle of suction surface. Two models of different blade thickness were modelled. The effect of blade thickness on the performance and internal flow characteristics of a single channel pump model was investigated by using computational fluid dynamics (CFD) method. By the change of blade thickness, it has been proven that the impeller blade thickness gives considerable effect on the performance and internal flow characteristics and relatively thinner blade thickness showed better performance at the almost whole operation condition in this study.

## 1. Introduction

The single channel pump is a kind of pump usually used for special usage. In industry or agriculture field, the main feature of the single channel pump is to operate in waste water condition without clogging for transportation of solid or solid-liquid mixing materials, because the impeller with periodic blades is quite easy to be blocked under these operation conditions. Moreover, sometimes in the fisheries or agriculture field, the transportation of alive fish, shrimp, fresh fruits or vegetables is needed. The damage of transportation substances need to be reduced as much as possible. The single channel pump is possible to meet with these requirements.

However, there are not so many previous studies related to the single channel pump. Because of the unique blade shape, the performance prediction needs to be carefully considered, and thus it is necessary to investigate the performance and internal flow characteristics of the single channel pump.

To evaluate the performance prediction accuracy of single channel pump under computational fluid dynamics, some research results are reported. Wu et al. [1] has employed various turbulence models to predict the performance of single channel pump. Keays et al. [2] did a study about the behaviour of a single blade waste-water pump using both of the

* Graduate school, Department of Mechanical Engineering, Mokpo National University
** Department of Mechanical Engineering, Institute of New and Renewable Energy Technology Research, Mokpo National University
† 교신저자, E-mail : ydchoi@mokpo.ac.kr

The KSFM Journal of Fluid Machinery: Vol. 23, No. 1, February 2020, pp.15~22(Received 13 Aug. 2019; revised 17 Dec. 2019; accepted for publication 19 Dec. 2019)
한국유체기계학회 논문집: 제23권, 제1호, pp.15~22, 2020(논문접수일자: 2019.08.13, 논문수정일자: 2019.12.17, 심사완료일자: 2019.12.19)

numerical and experimental methods. The study results revealed that the primary source of poor efficiency was caused by the separated region behind the trailing edge and the cut water area. Ji et al. [3] employed a partitioned FSI solution strategy to quantitatively obtain the coupling effects of a fluid–structure system in a single blade centrifugal pump on the unsteady flow. Litfin et al. [4] performed numerical simulations of two centrifugal pump impellers for wastewater application with three different trailing edge shapes.

In this study, two single chanel pump models, which has same design specification except for the impeller blade thickness, were designed and the effect of single channel pump blade thickness was investigated by computational fluid dynamics (CFD) analysis.

## 2. Design of single channel pump impeller and volute

Table 1 shows the design specification of the single channel pump model. Fig. 1(a) and (b) shows the three dimensional and two dimensional view of single channel pump model. The main dimensions of single channel pump model was calculated by referring some previous research results [5]. The blade of single channel pump model was modelled by establishing the pressure surface and suction surface. To construct the suction surface, a center line (Line 1) need to be drawn first. Then the suction surface can be established following Line 1. The Line 1 can be modified by changing $\beta_0$. When the blade suction surface shape is established, the blade pressure surface shape and pressure side outlet angle $\beta_2$ are fixed. As the outlet blade angles ($\beta_0$, $\beta_1$, $\beta_2$) of single channel pump model are very effective factors for the pump hydraulic performance and internal flow characteristics, the angles need to be carefully considered.

Table 1 Design specification

| Item | Nomenclature | value |
|---|---|---|
| Capacity coefficient | $\phi$ | 0.028 |
| Head coefficient | $\varphi$ | 0.368 |
| Rotational speed | $n$ ($rpm$) | 1470 |
| Impeller inlet-outlet diameter ratio | $D_{outlet}/D_{inlet}$ | 2.4 |

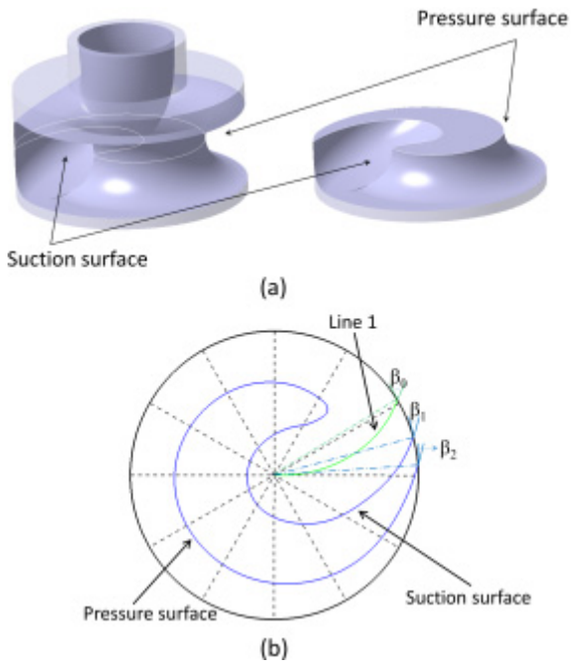


Fig. 1 3D modeling and schematic view of single channel pump model

In order to more deeply understand the Line 1, the explanation of the geometry relationship is presented in Fig. 2. The definition of the Line 1 is shown as Equation (1) and the parameter of m is determined as 2 [6]. The relationship among the three parameters ($\beta_0$, $\theta$, $\alpha_0$) can be found in Fig. 2.

In various quadrants, the geometry relationship can be written as Equations (2) and (3). In order to accurately understand the relationship between wrap angle ($\theta$) and outlet angle ($\beta_0$), the Equations (2) and (3) were solved by Matlab [7] and the solved result is shown in Fig. 3. In this study, some industrial application experiences and suggestions from some published books [5] were referred. If the wrap angle is

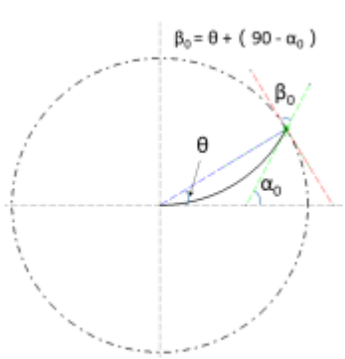


Fig. 2 Explanation of the geometry relationship

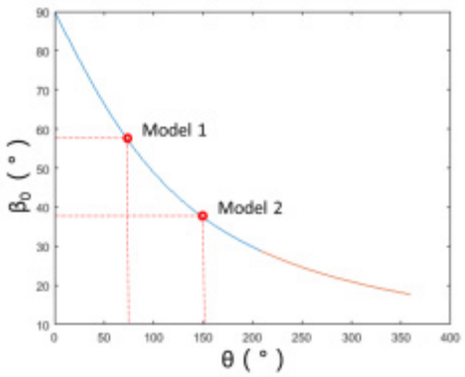


Fig. 3 Relationship between wrap angle and outlet angle

too large or too small, it could lead to trouble of three dimensional modeling and the decline of the hydraulic performance. For the application in industry field, the wrap angle within 180° was recommended to achieve a better pump performance. The outlet angle of $\beta_0$ =57°(Model 1) and $\beta_0$=37°(Model 2) were selected, the corresponding wrap angle were $\theta$=75°(Model 1) and $\theta$ =152°(Model 2).

$$r = a.\theta^m \tag{1}$$

where $r$ is polar radius and $a$ is a constant, $\theta$ is wrap angle and $m$ is power coefficient of wrap angle.

When $0^\circ < \theta < 270^\circ$, $(m=2)$

$$\beta_0 = \left|90 - \left|\arctan\left(\frac{m.\sin\theta + \theta.\cos\theta}{m.\cos\theta - \theta.\sin\theta}\right) - \theta\right|\right| \tag{2}$$

When $270^\circ < \theta < 360^\circ$, $(m=2)$

$$\beta_0 = \left|90 - \left|\arctan\left(\frac{m.\sin\theta + \theta.\cos\theta}{m.\cos\theta - \theta.\sin\theta}\right) - \theta + 180\right|\right| \tag{3}$$

After all the parameters were determined, the 3D modeling of single channel impeller models and the blade thickness distributions were established as shown in Fig. 4. The other main dimensions except for the blade thickness of the two models were kept in the same value. From the 3D modeling shape and blade thickness distribution, it can be seen that the blade thickness of the two single channel pump models are quite different. The blade thickness of Model 1 is

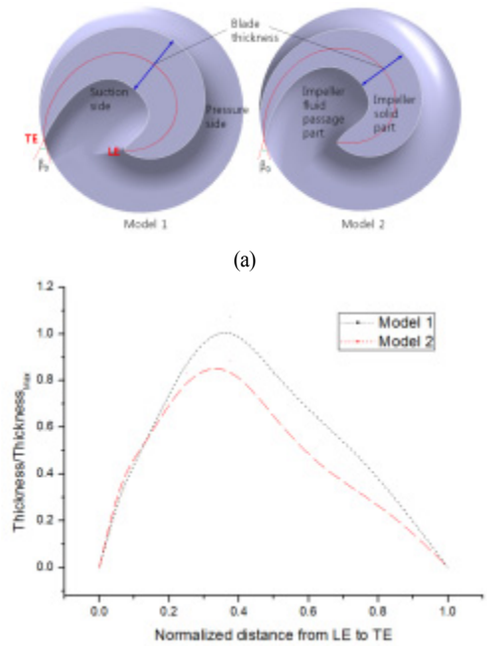


Fig. 4 3-D modeling and blade thickness distribution of the single chanel pump models

thicker than that of Model 2. Fig. 5 presents the cross section area distribution of the single channel pump volute. The cross section area distribution is a linear line, and the first cross section area (CSA-1) is designed relatively largely. As we know, the single channel pump is widely used for transport solid materials, if the first cross section area is too small, it is quite easy to be blocked.

## 3. Numerical methods

The fluid domain of the single channel pump geometry was modelled in 3D and the numerical grid

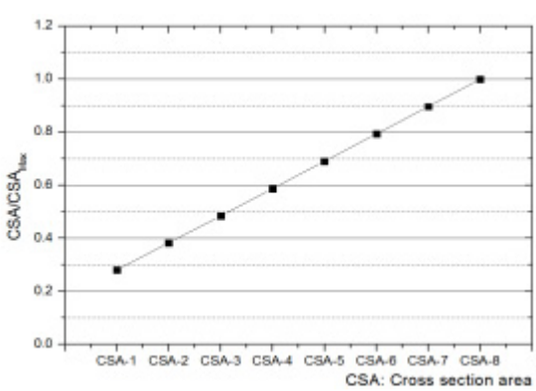


Fig. 5 Cross section area distribution of pump volute

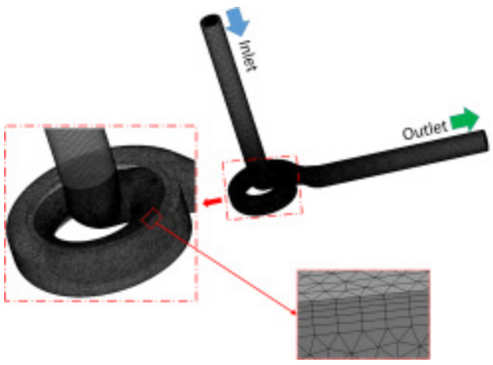


Fig. 6 Numerical grid

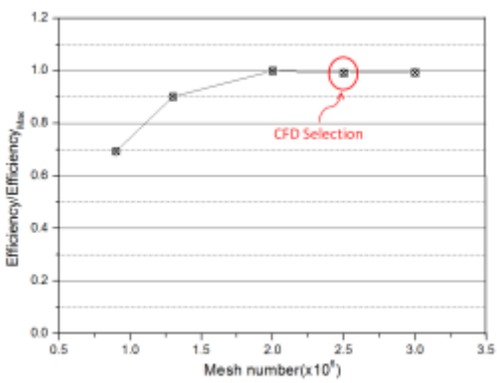


Fig. 7 Mesh dependence test

(Tetrahedral mesh) was generated as shown in Fig. 6. For a better prediction of single channel pump performance, the construction of numerical grid shape was elaborated to ensure the accuracy of the prediction results. The $y^+$ value of impeller was set below 10 and the mesh dependence test by Model 2 has been conducted as shown in Fig. 7. When the mesh number is larger than 2 million, the efficiency difference is within 1%. Therefore, a mesh number of 2.5million was selected to conduct the CFD analysis for the single channel pump model. For Model 1, only blade thickness is different from Model 2, so a similar mesh number was applied for it.

Moreover, The turbulence models of $k-\varepsilon$, $k-\omega$, *RNG* and *SST* are employed to do the turbulence model dependence test by Model 2, and the test results are presented in Fig. 8. The tendency of performance curves conducted by various turbulence models is similar and the shear stress transport turbulence (SST) model has been adopted in this study because of its superiority to estimate both separation and swirling flow on the wall of complex blade shapes.

The numerical methods and boundary condition are

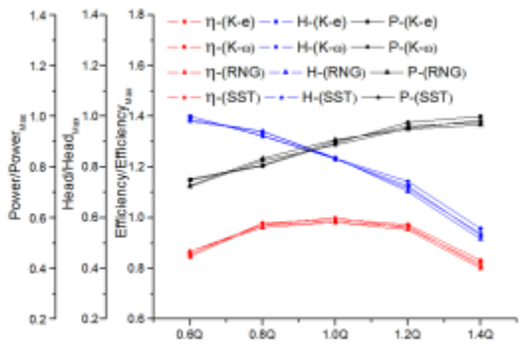


Fig. 8 Turbulence model dependence test

Table 2 Numerical methods and boundary condition

| | | |
|---|---|---|
| Numerical methods | Mesh type | Tetrahedral mesh |
| | Element number | $2.5\times10^6$ |
| | Cavitation model | Reyleigh-Plesset |
| | Fluid type | Water |
| | | Water vapor |
| | Turbulence model | *SST* |
| | Calculation type | Steady/Unsteady |
| Boundary condition | Rotor-stator interface | Frozen rotor |
| | Inlet of pump | Total pressure |
| | Outlet of pump | Mass flow rate |
| | Wall | No-slip |

summarized in Table 2. The CFD analysis was conducted by using ANSYS CFX [8]. The general connection at the rotational and fixed interfaces is set as frozen rotor and transient frozen rotor for both steady and unsteady state calculation. The total pressure and mass flow rate are applied at the inlet and outlet of the pump models, respectively. The cavitation model of Reyleigh-Plesset is adopted to implement the two-phase flow calculation of the single channel pump models.

## 4. Results and discussion

### 4.1 Performance curves of pump models

Considering only the hydraulic loss, the efficiency of single channel pump models are calculated by the following Equation (4):

$$\eta = \frac{\rho g H Q}{T\omega} \tag{4}$$

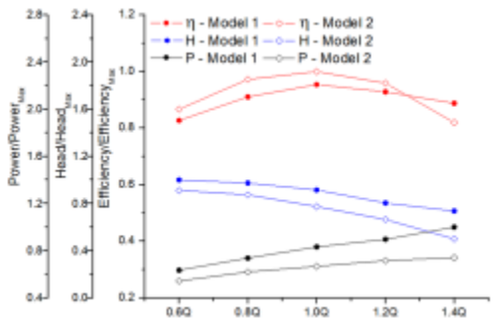


Fig. 9 Comparison of pump performance curves

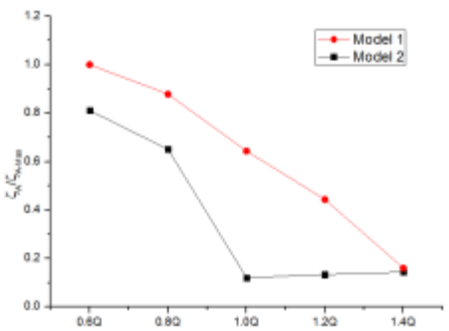


Fig. 10 Comparison of pressure fluctuation at the pump blade outlet by pump models

where $\eta$ is the efficiency; $T$ is the input torque; $\omega$ is the angular velocity; $\rho$ is the water density; $g$ is the gravitational acceleration; $Q$ is the flow rate and $H$ is the head of the pump models.

Fig. 9 presents the performance curves of pump Models 1 and 2. The efficiency of pump Model 2 is higher than that of Model 1 at the almost flow rate regions only except for the 1.4Q. However, The head and output power of the pump Model 1 are higher than those of the pump Model 2 in the whole flow rate region. The results show that the pump blade thickness gives considerable influence on the pump performance. It is conjectured that as the blade thickness changes, the blade loading on the blade surface varies, and then the head and output power receives the effect of the blade loading.

As the pressure fluctuation in the single channel pump is most vulnerable point of the pump in comparison with the other types of centrifugal pump, the quantitative averaged value of static pressure fluctuation around the impeller outlet on the plane of passage half width is calculated according to the variation of the pump flow rate as shown in Fig. 10. The averaged fluctuation of the static pressure $\zeta_A$ is defined and obtained by the Equation (5) as follows:

$$\zeta_A = 2\sqrt{\frac{1}{N}\sum_{1}^{n}(p-\bar{p})}/\rho u_2^2 \qquad (5)$$

where the $p$ is the static pressure, $\bar{p}$ is the averaged static pressure, $u_2$ is the tangential velocity at the periphery of impeller.

The static pressure fluctuation of Model 1 decreases almost linearly by the increase of flow rate. However, for Model 2, the static pressure fluctuation decreases by the increase of flow rate until the design point and it achieved a minimum value at the design point. Over the design flow rate region, the static pressure fluctuation increases slightly by the increase of the flow rate. Moreover, The values of the static pressure fluctuation for Model 2 much lower than those for Model 1 at the whole flow rate region. This result implies that the design of blade thickness gives remarkable effect on the pressure fluctuation in the pump and the pressure fluctuation can be efficiently controlled by a proper value of the blade thickness.

The turbulence kinetic energy is measured to investigate the intensity of turbulence in the pump models [9]. Higher turbulence kinetic energy might cause higher energy loss. Therefore, the turbulence kinetic energy distribution was utilized to estimate the turbulence intensity of single channel pump as shown in Fig. 11. It can be clearly observed that the relatively higher turbulence kinetic energy is mainly distributed around the blade leading edge and pressure side. The turbulence kinetic energy of Model 1 is higher than that of Model 2. It can be conjectured from the turbulence kinetic energy distribution that the lower efficiency in the pump Model 1 might be caused by the higher mixing loss resulted from the very complicated turbulence flow in the Model 1.

The streamline distributions of the assemblied impeller and volute at design point are illustrated in Fig. 12. It could be observed that there are swirling flows and flow separation existing around the leading edge of the blade. To more detailly investigate the flow pattern in this region, a mid-span cut plane was

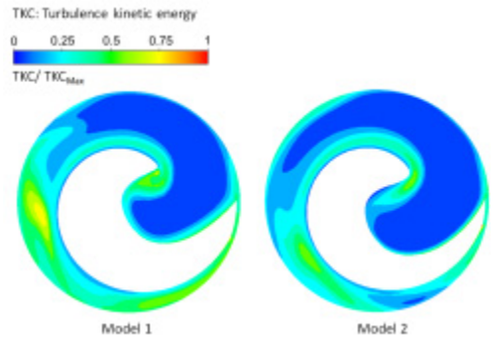


Fig. 11 Turbulence kinetic energy distribution at the design flow rate (1.0$Q$)

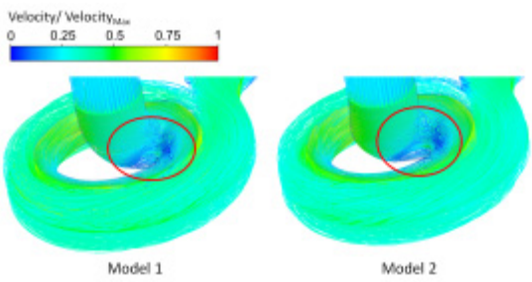


Fig. 12 Streamline distribution of the single channel pump (1.0$Q$)

inserted as shown in Fig. 13(b) and the surface streamline distribution is illustrated in Fig. 13(a). The swirling flow could be found in both of the two models and flow separation could be clearly observed at the

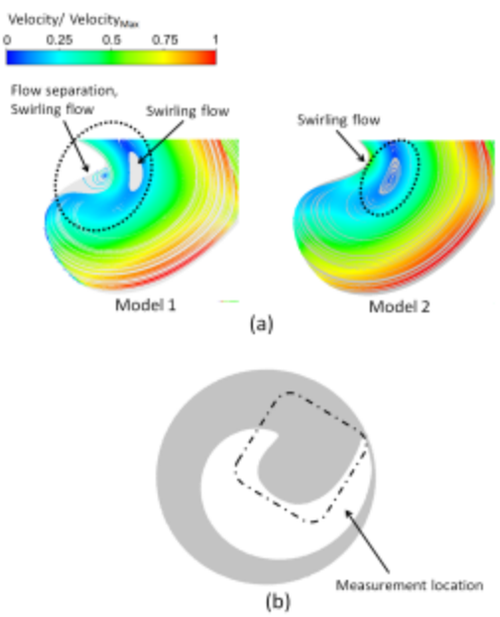


Fig. 13 Magnified view of surface streamline distribution at the mid-span plane (1.0$Q$)

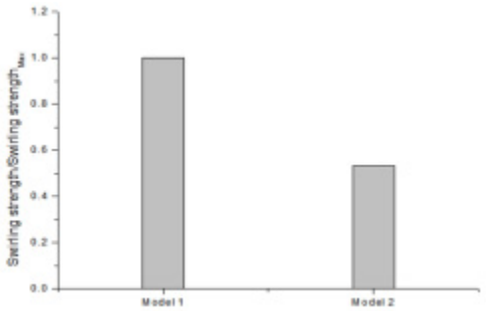


Fig. 14 Comparison of swirling strength at the mid-span plane (1.0$Q$)

leading edge of Model 1. As is known to all, the swirling flow and flow separation could lead to hydraulic loss and decrease the pump efficiency. Fig. 14 shows the quantified swirling strength at the mid-span cut plane of the two models. The swirling strength of Model 2 is much lower than Model 1.

For the single channel pump, the radial force needs to be investigated because it is quite important for the fluid induced vibration. Fig. 15 shows the transient radial force distribution of the pump impeller during one revolution. The radial force of Model 2 is smaller than Model 1 at the entire range of 360°. For both of the two models, the radial force distribution from 180° to 360 ° is larger than that from 0° to 180°.

## 4.2 Cavitation performance

Fig. 16 shows the comparison of suction performance of single channel pump models under various operation conditions by CFD analysis. The definitions of the head coefficient ($\varphi$) and cavitation number ($\sigma$) are shown as Equations (6) and (7):

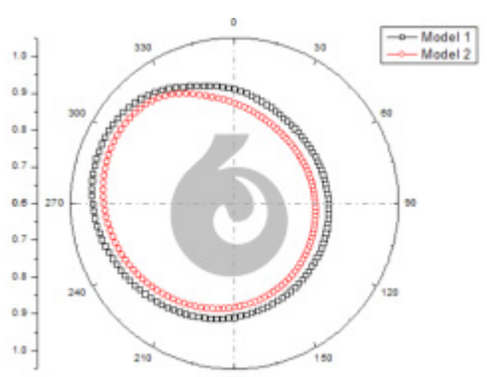


Fig. 15 Transient radial force of the impeller during one revolution (1.0$Q$)

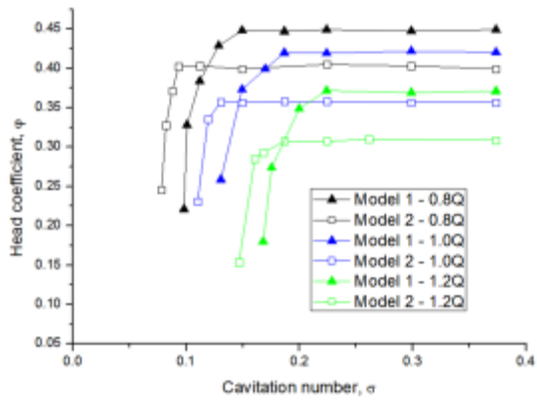


Fig. 16 Comparison of suction performance of single channel pump models by CFD analysis results

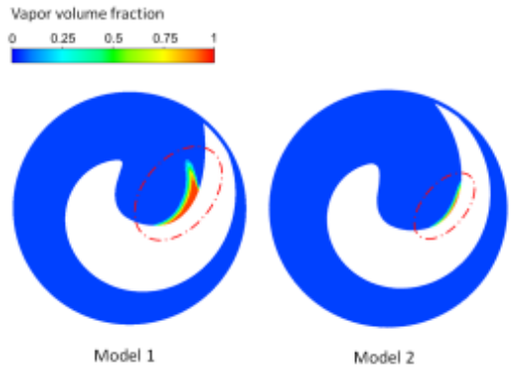


Fig. 17 Comparison of cavitation inception on the middle cut-plane (σ = 0.15, 1.0*Q*)

$$\varphi = \frac{H}{V_{tip}^2/2g} \tag{6}$$

$$\sigma = \frac{p - p_v}{\rho V_{tip}^2/2} \tag{7}$$

where $p$ is the static pressure at the pump inlet, $p_v$ is the vapor pressure, H is the effective head of the single channel pump and $V_{tip}$ is the impeller peripheral velocity.

According to the CFD analysis results illustrated in Fig. 16, the suction performance of the pump with impeller Model 2 is better than of the pump with impeller Model 1 at 0.8Q, 1.0Q and 1.2Q. Moreover, for the comparison of cavitation inception in the pump internal passage, vapor volume fraction (0: Pure water, 1: Cavitation inception) on the impeller middle cut-plane is presented as shown in Fig. 17. The cavitation phenomena usually occurs at the entrance of centrifugal pump impeller. However, in the single channel pump impeller, the cavitation occurrence location is wholly different from the usual centrifugal pump. It is recognized that the cavitation occurs in the middle of suction surface of single channel pump. The high volume fraction area locates in the vicinity of blade suction surface in both impeller models, furthermore, it is clear that the vapor volume fraction distribution of impeller Model 1 has much higher value with wider area in the impeller passage.

The reason of the higher suction performance by the pump with impeller Model 2 is inferred that the relatively larger outlet angle and wrap angle could influence the flow passage shape of single channel pump impeller. Therefore, the hydraulic and cavitation performance could be affected.

## 5. Conclusion

In this study, the effect of blade thickness on the performance and internal flow characteristics of single channel pump model has been analyzed verified by using computational fluid dynamics (CFD) method.

A thin blade thickness showed a better efficiency at the main operation conditions than the thick blade thickness of single channel pump.

The static pressure fluctuation of thin impeller blade is lower than that of thick impeller blade. And the thin impeller blade achieved a minimum pressure fluctuation of single channel pump at the design point. Moreover, the high turbulence kinetic energy intensity is mainly distributed around the outlet of blade pressure side and leading edge. The turbulence kinetic energy intensity of thin impeller blade was lower than that of thick impeller blade. The swirling flow strength of thin blade is much lower than the thick blade. Moreover, the impeller radial force of thin blade is lower than the thick blade at the entire range of one revolution.

The head drop tendency of single channel pump models by cavitation number is similar to that of normal centrifugal pump. The cavitation is easier to occur at higher flow rate by decreasing the cavitation number. The impeller of Model 2 with thinner blade thickness showed much better suction performance than the impeller of Model 1 at 0.8Q, 1.0Q and 1.2Q.

The hydraulic and cavitation performance could be greatly affected by different blade thickness. Therefore, it is quite important to determine a appropriate blade thickness to achieve a better pump performance.

## References


(1) X Wu, H Liu, J Ding, 2006 "Performance prediction of single-channel centrifugal pump with steady and unsteady calculation and working condition adaptability for turbulence model", Transactions of the Chinese Society of Agricultural Engineering, Vol.220, Part E, pp. 85-91.

(2) J Keays, C Meskell, 2017 "A study of the behaviour of a single-bladed waste-water pump", Journal of Process Mechanical Engineering, Vol.33, Supp.1, pp. 79-87.

(3) J Pei, S Yuan, J Yuan, 2013 "Fluid-structure coupling effects on periodically transient flow of a single-blade sewage centrifugal pump" Journal of Mechanical Science and Technology, Vol.27, No.7, pp 2015-2023.

(4) O. Litfin, A. Delgado, K. Haddad, H. Klein, 2017 "Numerical and experimental investigation of trailing edge modifications of centrifugal wastewater pump impellers". Proceedings of the ASME 2017 Fluids Engineering Division Summer Meeting, Hawaii, USA.

(5) X. Guan, 2011 "Modern pump theory and design", Beijing, China astronautic publishing house.

(6) D Yuan, X Cong, 2006 "Research on the design method of double-flow-passage impeller" Drainage and irrigation machinery, Vol.24, No.1, pp 17-18.

(7) Matlab Inc., Matlab Documentation, Ver. 2016a, http://www.Matlab.com, Accessed, 2019.

(8) ANSYS Inc., ANSYS CFX Documentation, Ver. 18.1, http://www.ansys.com, Accessed, 2019.

(9) S. B. Pope, 2000 "Turbulent flows", Cambridge, Cambridge University Press.